

L. Z. Zeng
Graduate Research Assistant.

J. F. Klausner
Assistant Professor.

Department of Mechanical Engineering,
University of Florida,
Gainesville, FL 32611

Nucleation Site Density in Forced Convection Boiling

Measurements of nucleation site density, n/A , have been obtained for forced convection boiling of refrigerant R113 in a horizontal 25 × 25 mm i.d. square transparent test section with a nichrome heating strip. It has been found that the behavior of the nucleation site density is significantly different from that found in pool boiling. The mean vapor velocity, heat flux, and system pressure appear to exert a strong parametric influence. It is demonstrated that although the nucleation site density is dependent on the critical cavity radius, r_c , it is not sufficient for correlating n/A .

Introduction

The heat transfer associated with forced convection boiling is typically treated as resulting from two distinct and additive contributions as suggested by Rohsenow (1952): that due to bulk turbulence and that due to the ebullition process. Chen (1966) coined the term macroconvection to designate the transport of heat from the heating surface due to the bulk turbulent motion of the two-phase mixture and the term microconvection to designate that portion of heat transport associated with the incipience, growth, and departure of vapor bubbles. Chen (1966) subsequently proposed the following flow boiling heat transfer relation:

$$h_{2\phi} = Eh_l + Sh_b \quad (1)$$

where $h_{2\phi}$ is the flow boiling heat transfer coefficient, h_l is the single-phase heat transfer coefficient due to the liquid fraction flowing, h_b is the heat transfer coefficient appropriate for nucleate pool boiling, E is an amplification factor to account for increasing bulk turbulence with increasing vapor quality, and S is a suppression factor to account for the effective superheat seen by growing vapor bubbles during flow boiling. Here, Eh_l is the heat transfer contribution due to macroconvection while Sh_b is that due to microconvection. Numerous flow boiling heat transfer correlations have since been proposed that follow the same basic form as Eq. (1), many of which have been tested by Gungor and Winterton (1986). None of these correlations can satisfactorily correlate all of the flow boiling heat transfer data available in the literature. Klausner et al. (1992a) have demonstrated that the bubble departure mechanism for pool and flow boiling can be significantly different, depending on flow conditions, thus casting doubt on Chen's (1966) formulation of the microconvective component of heat transfer. In order to model the microconvection component of heat transfer in flow boiling reliably, detailed information on the incipience, growth, and departure of vapor bubbles is required. This work is specifically concerned with nucleation site density in forced convection boiling.

Due to its governing influence on heat transfer, the nucleation site density has been the focus of numerous investigations for pool boiling (Clark et al., 1959; Griffith and Wallis, 1960; Kurihara and Meyers, 1960; Gaertner and Westwater, 1960; Hsu, 1962; Gaertner, 1963, 1965; Nishikawa et al., 1967; Singh et al., 1976). The general consensus from these investigations is that the formation of nucleation sites is highly dependent on surface roughness, geometry of microscopic scratches and pits on the heating surface, the wettability of the fluid, the amount of foreign contaminants on the surface, as well as the

material from which the surface was fabricated. Due to the large number of variables that are difficult to control, none of these investigators were successful in developing a general correlation for nucleation site density. Griffith and Wallis (1960) suggested that for a given surface the critical cavity radius, r_c , is the only length scale pertinent to incipience provided the wall superheat is uniform. Although they recognized the wall superheat is nonuniform in pool boiling, they used r_c to correlate the nucleation site density as follows:

$$\frac{n}{A} = C_1 \left(\frac{1}{r_c} \right)^m \quad (2)$$

where n/A is the nucleation site density, C_1 and m are empirically determined constants, and when $\rho_l \gg \rho_v$

$$r_c = \frac{2\sigma T_{\text{sat}}}{\rho_v h_{fg} \Delta T_{\text{sat}}} \quad (3)$$

where T_{sat} is the saturation temperature, σ is the surface tension, h_{fg} is the latent heat of vaporization, and $\Delta T_{\text{sat}} = T_w - T_{\text{sat}}$ is the wall superheat.

Nucleation site density data of Griffith and Wallis (1960) for pool boiling of water on a copper surface are shown in Fig. 1 as a function of ΔT_{sat} . For $n/A < 4 \text{ cm}^{-2}$ the nucleation site density increases smoothly with increasing ΔT_{sat} . However, for $n/A > 4 \text{ cm}^{-2}$ no correlation exists between n/A and ΔT_{sat} . Moore and Mesler (1961) used a fast response thermocouple to demonstrate that the heating surface temperature directly beneath a nucleation site in pool boiling experiences rapid fluctuations. Recently Kenning (1991) used thermochromic liquid crystals to measure the spatial variation of wall superheat with pool boiling of water on a 0.13-mm-thick stainless steel heater. It was demonstrated that the wall superheat was very nonuniform and $|\Delta T'_{\text{sat}}|/\Delta T_{\text{sat}}$ varied from 0.25 to 1.5 over a distance of a few mm, where an overbar implies an ensemble spatial average and a prime denotes a spatial variation from the mean. Using a conduction analysis, it was also shown that in the presence of ebullition, spatial nonuniformities of wall superheat on the surface of "thick plates" may also be significant depending on geometry and thermal conductivity of the plate. Kenning's (1991) result suggests that a microlength scale, which is related to the spatial temperature field, may also be important in characterizing incipience of vapor bubbles. According to the suggestion of Eddington et al. (1977) and the experimental findings of Calka and Judd (1985), at low n/A where nucleation sites are sparsely distributed, neighboring nucleation sites do not interact thermally. However, at large n/A where nucleation sites are closely packed, thermal interference among neighboring sites exists. Since it has been demonstrated that ΔT_{sat} is highly nonuniform in the presence of nucleation sites, a question arises as to whether at large n/A the average wall superheat is sufficient for characterizing the

Contributed by the Heat Transfer Division for publication in the JOURNAL OF HEAT TRANSFER. Manuscript received by the Heat Transfer Division March 1992; revision received August 1992. Keywords: Boiling, Forced Convection. Associate Technical Editor: L. C. Witte.

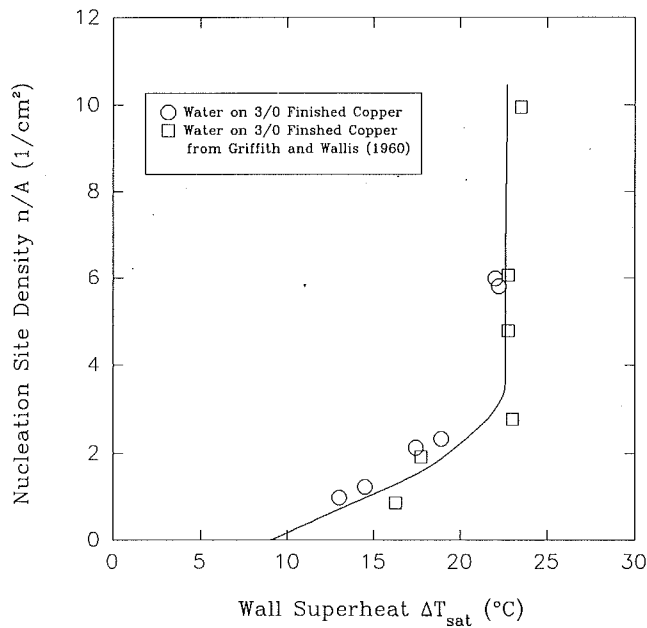


Fig. 1 Pool boiling nucleation site density data from Griffith and Wallis (1960)

local wall superheat experienced by individual nucleation sites. The data displayed in Fig. 1 suggest that it is not.

Few similar studies on nucleation site density in flow boiling have been reported. In one such investigation Eddington and Kenning (1978) measured the nucleation site density with subcooled flow boiling of water for a narrow range of flow conditions. It was suggested that n/A is related to r_c . The objectives of the present work are twofold: (1) to study the influence of flow and thermal conditions on the nucleation site density in saturated forced convection boiling, and (2) determine whether or not the nucleation site density in flow boiling is solely a function of the critical radius, r_c , as has been suggested for pool boiling. Measurements of nucleation site density have been obtained for flow boiling of refrigerant R113 in a 25×25 mm i.d. square transparent tube. These measurements have been obtained for the isolated bubble regime with stratified flow. In general, the liquid/vapor interface was wavy and periodic slugs of liquid were observed passing through the test section. No flow regime transitions were observed. The liquid phase Reynolds number based on the mean velocity ranged from 12,000 to 27,000 and that for the vapor phase ranged from 24,000 to 80,000. The flow conditions are characterized by the mass flux, G , liquid film thickness, δ , vapor quality, x , mean liquid velocity u_l , and mean vapor velocity, u_v . Thermal conditions are characterized by the heat flux, q_w , the wall superheat, ΔT_{sat} , and saturation conditions (saturation temperature, T_{sat} , or saturation pressure, P_{sat}). The controllable inputs of the flow boiling facility are: G , x , P_{sat} (or T_{sat}), and q_w . Of the flow parameters considered, only two are independent since the mean liquid and vapor velocities were respectively calculated from

$$u_l = \frac{G(1-x)D}{\rho_l \delta} \quad (4)$$

and

$$u_v = \frac{GxD}{\rho_v(D-\delta)} \quad (5)$$

where D is the inside dimension of the horizontal square test section for which only the lower surface is covered with a liquid film. Therefore, when investigating the influence of one of the flow parameters on nucleation site density at constant saturation conditions, only one other flow parameter could be held constant, which introduced complexities in interpreting the data. The range of flow and thermal parameters covered in this work, which to a large extent were governed by the ability to visualize nucleation sites, are as follows: $G = 125$ – 290 kg/m²-s, $u_v = 1.6$ – 4.7 m/s, $u_l = 0.35$ – 0.68 m/s, $\delta = 3.5$ – 9.5 mm, $q_w = 14.0$ – 23.0 kW/m², $\Delta T_{sat} = 13.0$ – 18.0 °C, and $T_{sat} = 55.0$ – 75.0 °C.

Experimental Facility

The experimental facility in which flow boiling measurements of nucleation site density were obtained is shown schematically in Fig. 2. The refrigerant R113 forced convection boiling facility has been designed specifically to allow for flow visualization. A variable speed model 221 Micropump is used to pump R113 through the facility. The volumetric flow rate of refrigerant through the facility is monitored with an Erdco Model 2521 vane type flow meter equipped with a 4–20 mA analog output. Calibration of the flow meter demonstrates that it is accurate to within ± 0.5 percent of full scale, which is the repeatability claimed by the manufacturer. At the outlet of the flow meter, five preheaters, each of which has a maximum heat rate of 5 kW, have been installed. Each preheater consists of a 25.4 mm i.d., 1.2-m-long hard copper pipe around which 18 gage nichrome wire has been circumferentially wrapped. The nichrome wire is electrically insulated from the copper pipe with ceramic beads. The heaters are thermally insulated with 25.4-mm-thick fiberglass insulation. The voltage inputs to the preheaters are controlled with five 240 volt a-c autotransformers. The heat loss from the preheaters as a function of temperature difference between the insulation outer surface and ambient air has been predetermined from calibration.

A horizontal flow boiling visual test section is located downstream of the preheaters. A capacitance based liquid film thickness sensor, described in detail by Klausner et al. (1992b) has been installed on either side of the test section. The main body of the test section is comprised of a 25×25 mm inner dimension square pyrex tube that is 4 mm thick and 0.457 m long. A 0.13-mm-thick and 22-mm-wide nichrome strip, used for heating, has been attached to the lower inside surface of the square tube with epoxy. Six equally spaced 36 gage type E thermocouples have been attached to the back side of the nichrome strip using high thermal conductivity epoxy. In order to avoid biased temperature readings caused by a "fin effect," the thermocouple leads were also attached to the back of the heating strip over a length of at least 7 cm before being exposed

Nomenclature

D = square test section inner dimension, m
 G = mass flux, kg/m²-s
 h_{fg} = latent heat of vaporization, J/kg-K
 n/A = nucleation site density, 1/cm²
 r_c = critical cavity radius, m

T_{sat} = saturation temperature, °C or K
 ΔT_{sat} = wall superheat = $T_w - T_{sat}$, °C
 u = mean velocity, m/s
 x = vapor quality

δ = liquid film thickness, m or mm
 ρ = density, kg/m³
 σ = surface tension, N/m

Subscripts

l = liquid
 v = vapor

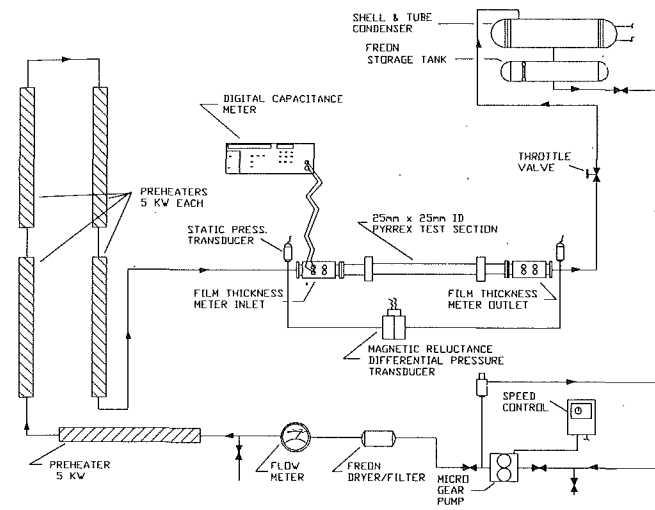


Fig. 2 Schematic diagram of flow boiling facility

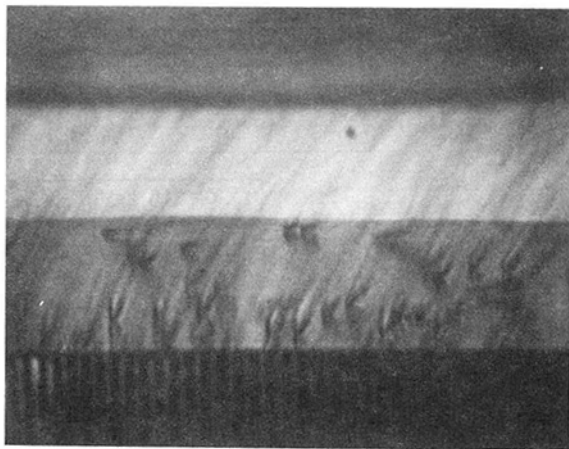


Fig. 3 Typical photograph of nucleation site density

to ambient air. The thermocouples are accurate to within $\pm 0.5^\circ\text{C}$ and measurements are repeatable to within $\pm 0.1^\circ\text{C}$. A conduction analysis showed that the temperature difference between the upper and lower surface of the heating strip is within 0.1°C for the maximum heat flux investigated and is within the repeatability of the thermocouples. A similar test section was fabricated in which the underside of the nichrome strip was coated with cholesteric liquid crystals. In order to heat the strip, a 36 volt, 120 amp d-c power supply has been electrically connected across the brass blocks with 2 gage cable.

Viatran model 2416 static pressure transducers have been installed at the inlet and outlet of the test section to measure the saturation pressure. They have an accuracy of ± 0.5 percent of full scale (30 psig). All bulk temperature and exterior temperature measurements are made with type E thermocouples. All analog signals have been input to an Access 12 bit digital data acquisition system, which consists of two 16-channel multiplexer cards with programmable gain from 1 to 1000. The multiplexer cards are interfaced with an 8-channel, 12-bit analog to digital (A/D) converter, which was mounted in an AT style personal computer.

The nucleation site density was measured optically with a digital imaging facility. The facility consists of a Videk Megaplus CCD camera with 1320×1035 pixel resolution. The CCD camera is equipped with a Vivitar 50 mm macro lens with high resolution and low optical distortion. The output of the CCD camera is input to an Epix 4 megabyte framegrabber. The framegrabber allows for either high resolution (1320×1035) or low resolution (640×480) imaging. Due to

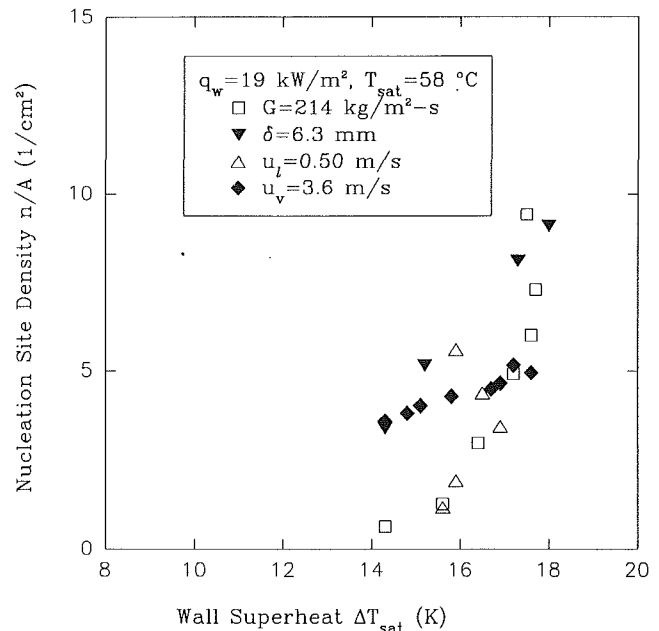


Fig. 4 Nucleation site density as a function of wall superheat for constant heat flux and saturation temperature

the wavy interface of the two-phase mixture it is not possible to observe the nucleation sites clearly from a view normal to the heating surface. Therefore, the nucleation sites must be viewed through the side wall of the test section through the liquid film. A typical image of nucleation sites is displayed in Fig. 3. Images are displayed on a Sony analog monitor with 1000 lines per inch resolution, and may also be printed on a Hewlett Packard Laser Jet III laser printer. Only nucleation sites within a 1.4-cm-wide by 2.2-cm-long area located at the center of the strip were counted. The nucleation site density measured from an ensemble average of 50 images was compared against that based on an average of ten images; identical results were obtained. Therefore, all nucleation site density measurements reported herein are based on an ensemble average of ten images. Presumably intermittent sites are accounted for. The problem of hysteresis was avoided by measuring nucleation site density only for increasing heat flux and increasing vapor velocity.

Experimental Results

Nucleation site density measurements have been obtained for a constant heat flux, $q_w = 19 \text{ kW/m}^2$, and saturation temperature, $T_{\text{sat}} = 58^\circ\text{C}$, over a range of flow conditions in which either the mass flux, G , liquid film thickness, δ , liquid velocity, u_l , or vapor velocity, u_v , was maintained constant. The nucleation site density, n/A , is shown as a function of wall superheat, ΔT_{sat} , in Fig. 4. The n/A data are not well correlated with ΔT_{sat} . In light of Fig. 1 and Eqs. (2) and (3), the behavior of n/A with ΔT_{sat} is considered to be anomalous. In order to demonstrate that the observed behavior is not simply due to experimental error, pool boiling nucleation site density data were obtained using the current facility by filling the test section with liquid and heating the nichrome surface while the circulation pump was off. Therefore the only net flow was induced by natural convection currents. The data are displayed in Fig. 5 as a function of both ΔT_{sat} and q_w . It is seen that n/A increases smoothly with both ΔT_{sat} and q_w in a similar fashion to the data shown in Fig. 1. As seen from Fig. 4, parameters other than ΔT_{sat} alone appear to exert an influence on n/A .

In order to examine the influence of the flow parameters on n/A , the nucleation site density is first plotted against vapor

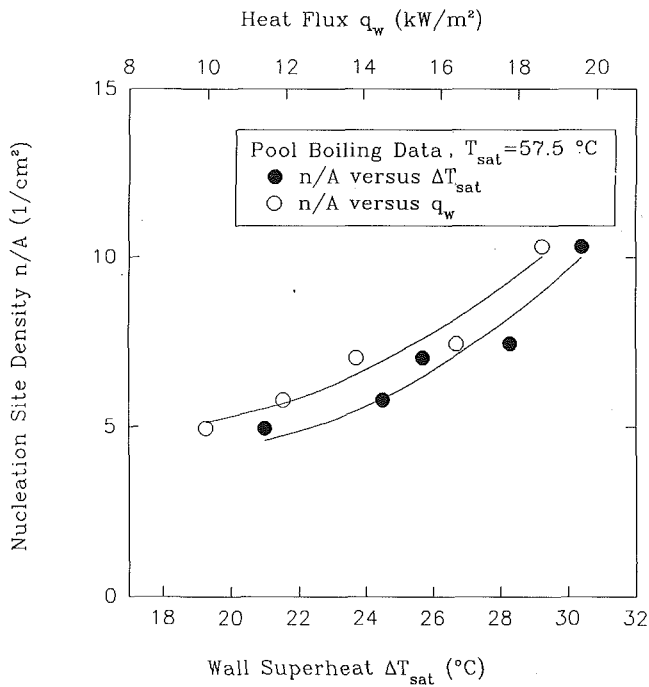


Fig. 5 Pool boiling nucleation site density as a function of wall superheat

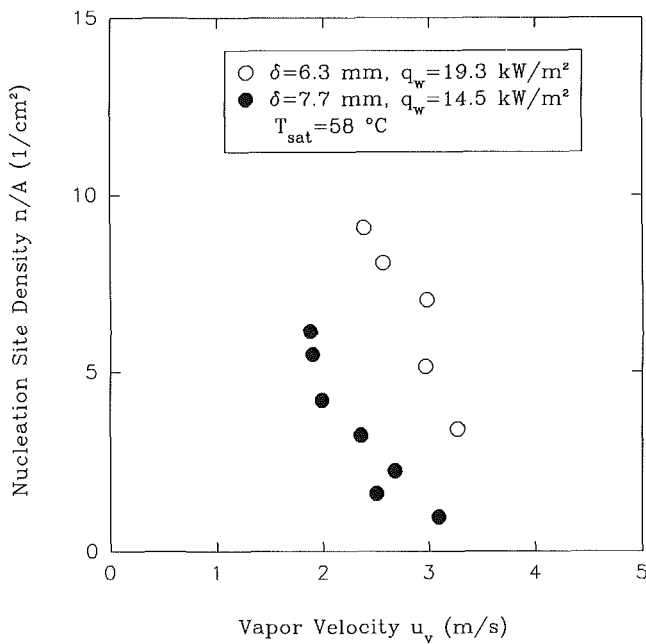


Fig. 6 Nucleation site density as a function of vapor velocity for constant heat flux and liquid film thickness

velocity at a fixed heat flux, q_w , and fixed liquid film thickness, δ , as shown in Fig. 6. It is seen that n/A decreases markedly with increasing vapor velocity, u_v . At a fixed heat flux, liquid film thickness, and saturation conditions, the data appear to fall on a single curve. As the heat flux is increased the curve shifts toward higher nucleation site density. Therefore, when investigating the influence of the flow parameters on n/A the heat flux will be maintained constant. Upon examination of Eqs. (4) and (5) it is possible that the trend shown in Fig. 6 is due to either increasing G or u_l instead of increasing u_v . To sort out whether G , u_v , or u_l has a controlling influence on n/A , Figs. 7 and 8 have been prepared. In Fig. 7, n/A is shown to increase with increasing G when u_l when q_w are fixed, but

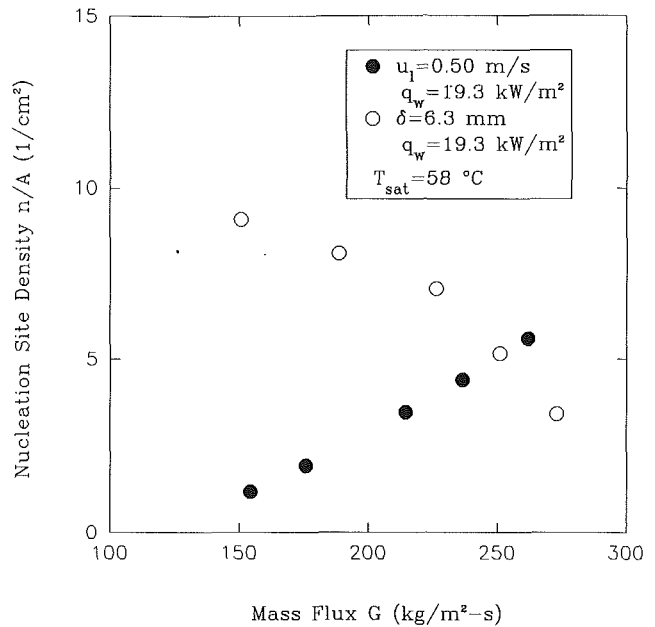


Fig. 7 Nucleation site density as a function of mass flux

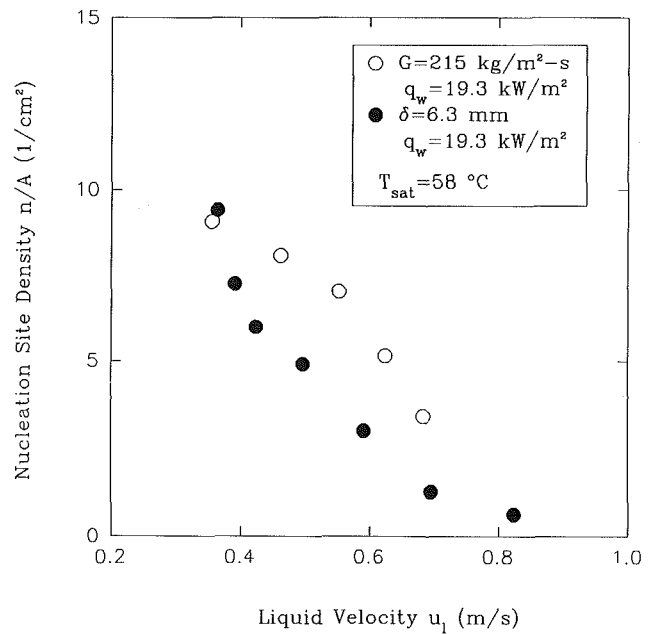


Fig. 8 Nucleation site density as a function of liquid velocity

decreases with increasing G when δ and q_w are fixed, and thus it appears that parameters other than G are controlling n/A . In Fig. 8 n/A is shown to decrease with increasing u_l for fixed G and q_w . When δ and q_w are fixed, n/A also decreases with increasing u_l , but the curve shape is significantly different. When comparing Figs. 6 and 8 it appears that n/A is better behaved when displayed as a function of u_v . Further evidence of this supposition is provided in Fig. 9 where n/A is displayed as a function of u_v for $q_w = 19.5 \text{ kW/m}^2$, $T_{\text{sat}} = 58^\circ\text{C}$, $G = 215 \text{ kg/m}^2\text{-s}$, and $u_l = 0.58$ and 0.49 m/s . It is seen that all of the data approximately fall on a single curve, thus demonstrating the governing influence of the mean vapor velocity on nucleation site density. The liquid film thickness δ is also shown as a function of u_v . Thus, the effect of liquid film thickness on n/A is also included in Fig. 9. Therefore, it is necessary to investigate the influence of δ on n/A .

In pool boiling, Nishikawa et al. (1967) demonstrated that

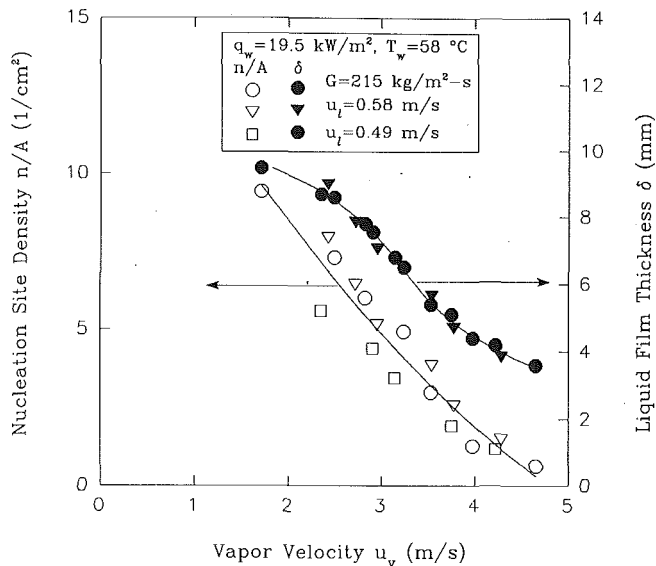


Fig. 9 Nucleation site density and liquid film thickness as a function of vapor velocity for constant heat flux and either constant mass flux or constant liquid velocity

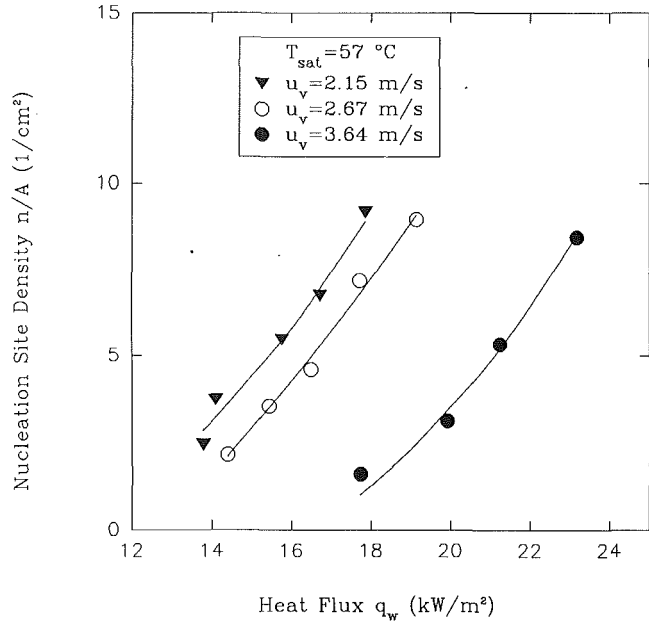


Fig. 11 Nucleation site density as a function of heat flux

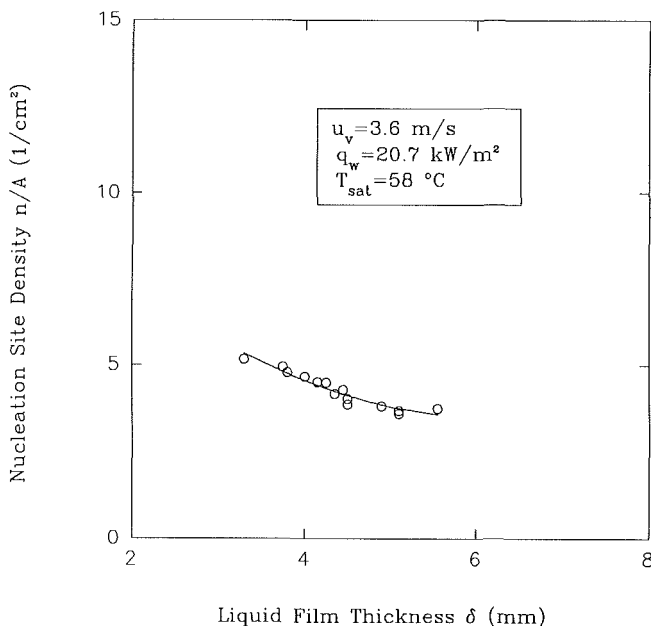


Fig. 10 Nucleation site density as a function of liquid film thickness

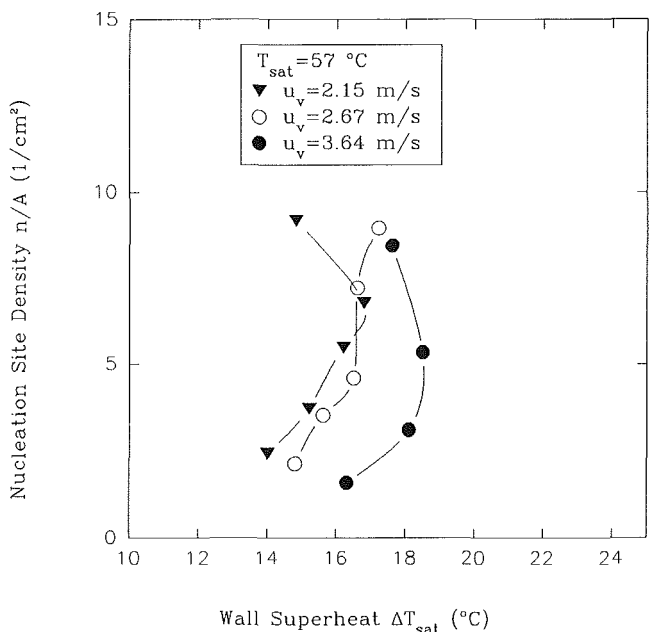


Fig. 12 Nucleation site density as a function of wall superheat

the nucleation site density increases with declining liquid film thickness. Mesler (1976) postulated that the same behavior should follow for flow boiling and used it to explain the measured increase in flow boiling heat transfer coefficient with declining liquid film thickness for stratified or annular flow. To the best of the authors' knowledge direct evidence supporting or refuting Mesler's claim has yet to be presented. To sort out the direct influence of liquid film thickness on nucleation site density, Fig. 9 suggests that it is necessary to maintain a fixed u_v , q_w , and T_{sat} . Figure 10 shows n/A as a function of liquid film thickness at $u_v = 3.58$ m/s, $q_w = 20.7$ kW/m², and $T_{sat} = 58$ °C. It is seen that indeed n/A increases with declining film thickness, which tends to support Mesler's claim regarding n/A as a function of film thickness, provided that u_v , q_w , and T_{sat} are fixed. However, over the range of film thickness investigated (3–6 mm) the increase in n/A is only marginal. Because n/A was obtained using a visualization technique,

it was not possible to obtain data for $\delta < 3$ mm. As $\delta \rightarrow 0$ the behavior of n/A is uncertain. To determine whether u_v or δ has a stronger influence on n/A , Fig. 9 is re-examined where it is seen that n/A decreases with decreasing δ , which is due primarily to increasing u_v . Therefore, it appears that u_v has a governing influence on the nucleation site density. An explanation and significance of this finding will be discussed later.

When testing the influence of thermal conditions on n/A , it is necessary to control u_v . In Fig. 11, n/A is shown as a function of q_w for three different values of u_v at $T_{sat} = 57$ °C. It is seen that at a fixed u_v , n/A increases smoothly with increasing q_w . As u_v increases, the curves shift toward decreasing n/A . The trends are consistent with those in Fig. 6. The n/A data from Fig. 11 are shown as a function of ΔT_{sat} in Fig. 12. The data display an anomalous behavior similar to that in Fig. 4.

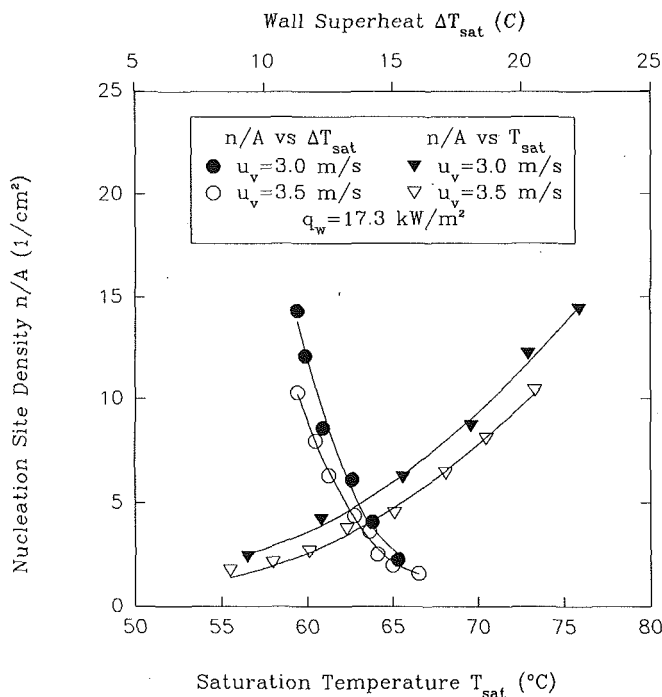


Fig. 13 Nucleation site density as a function of saturation temperature

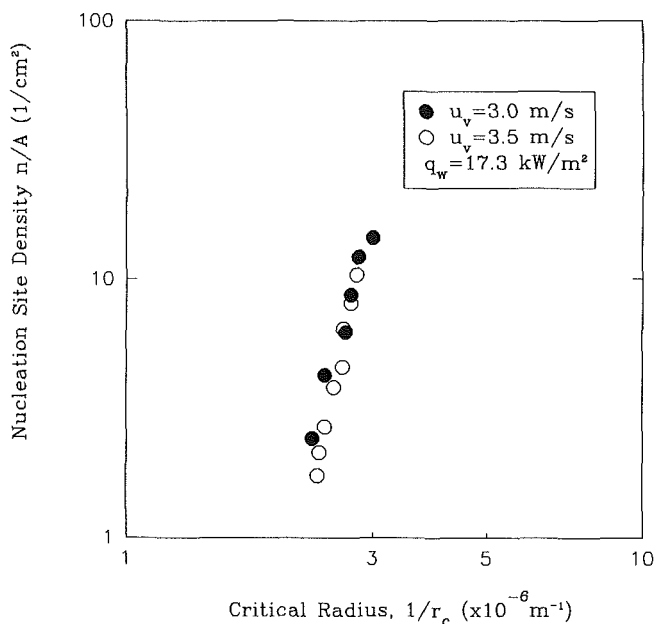


Fig. 14 Nucleation site density as a function of critical radius for constant heat flux and vapor velocity

To examine the dependence of n/A on the critical radius, it was decided that a constant heat flux would be maintained, and r_c would be controlled by raising the system pressure. Doubling the system pressure has the effect of essentially doubling the vapor density and increasing T_{sat} by several percent. The nucleation site density was measured for fixed u_v and q_w in which T_{sat} increased by 20°C by raising the system pressure from 1.3 to 2.3 bars. From these data Figs. 13 and 14 have been prepared. It is seen from Fig. 13 that ΔT_{sat} decreases with increasing T_{sat} . Nevertheless, n/A increases due to a decrease in r_c . This can be seen from Fig. 14, which shows increasing n/A with increasing $1/r_c$. Because the only physically sound explanation for the increase in n/A with increasing T_{sat} is due to a decrease in r_c , these data suggest that r_c is an important

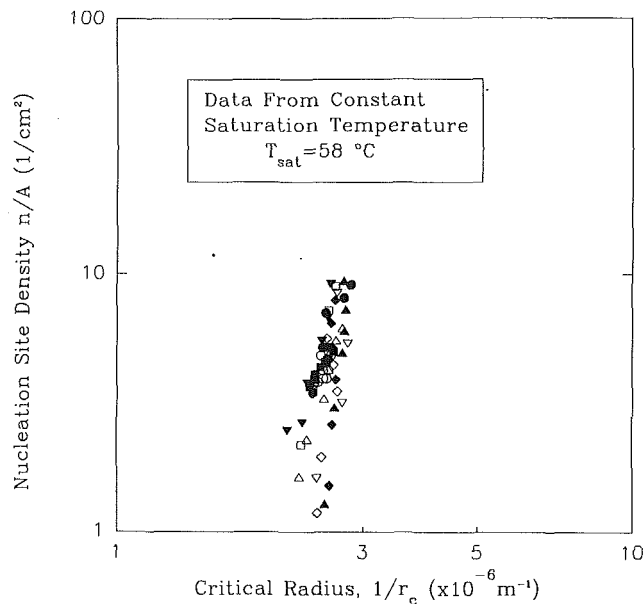


Fig. 15 Nucleation site density as a function of critical radius for all the flow boiling data

parameter in characterizing flow boiling nucleation site density.

Discussion of Results

Although the data in Fig. 14, as well as theoretical considerations, suggest that r_c is an important correlating parameter for flow boiling nucleation site density, it is by itself insufficient for correlating n/A . In Fig. 15, all the nucleation site density measurements obtained in this study, for $T_{sat} = 58^\circ\text{C}$, are displayed as a function of r_c . Although the data appear to be collapsed, a correlation in the form of Eq. (2) would not be useful due to the steepness of the slope. The pool boiling nucleation site density data of Griffith and Wallis (1960) display a similar behavior for large n/A .

In an attempt to understand this behavior, consideration is first given to the pool boiling analysis of Hsu (1962) in which it was demonstrated that the nonuniform liquid temperature field seen by a vapor embryo attempting to grow is important when considering incipience criteria. If a linear temperature profile is assumed for the liquid layer, a minimum cavity radius required for incipience may be expressed solely as a function of either ΔT_{sat} or q_w , provided properties are maintained constant. The data displayed in Fig. 4 show that ΔT_{sat} or q_w alone are insufficient for correlating flow boiling n/A data. Bergles and Rohsenow (1964) attempted a similar analysis for flow boiling, and the assumption of a linear temperature profile can also lead to the definition of a critical cavity radius that is solely dependent on ΔT_{sat} or q_w , provided properties are maintained constant. One shortcoming in these analyses is the assumption of a linear temperature profile in the liquid thermal layer. Certainly, the strength of the heat flux as well as that of the bulk turbulence will have a strong influence on the shape of the thermal layer. Nevertheless, these analyses suggest that in addition to the critical cavity radius based on Eq. (3), a length scale related to the thermal layer thickness may also be important in characterizing n/A .

In addition, it is emphasized that r_c has been calculated using Eq. (3) taking the wall superheat to be the average value, $\overline{\Delta T_{sat}}$. As mentioned earlier, Kenning (1991) used liquid crystal thermography to show that $|\Delta T'_{sat}|/\overline{\Delta T_{sat}}$ could be as large as 1.5 for pool boiling. In this study the liquid crystal boiling test section was used in conjunction with a Panasonic video recorder to record the flow boiling temperature field of the

heating surface for the following flow and thermal conditions: $u_v = 3.0$ m/s, $q_w = 18.1$ kW/m², and $T_{\text{sat}} = 58.3^\circ\text{C}$. It was found the temperature field was very nonuniform in both space and time and $|\Delta T'_{\text{sat}}|/\Delta T_{\text{sat}}$ was as large as 0.5. Therefore, it appears that the average wall superheat is insufficient for characterizing the local wall superheat experienced by individual nucleation sites.

The data presented thus far satisfy the objectives of this work: (1) Of the flow and thermal parameters investigated, u_v , q_w , and T_{sat} appear to have a governing influence on n/A . (2) By itself, r_c is not sufficient for correlating n/A . Pool boiling n/A correlations based on r_c are not applicable to flow boiling.

The above results raise a fundamental question: What is the physical basis for the apparently strong influence of u_v and q_w on n/A ? Unfortunately, with the experimental technique employed in this investigation, a conclusive answer to this question is out of reach. Some insight is gained by considering that bulk turbulence in stratified two-phase flow is largely dependent on interfacial waves. The interfacial shear stress is the means by which wave information is communicated to the liquid film. Andritsos and Hanratty (1987) have provided extensive experimental evidence that the mean vapor velocity is a controlling parameter on the interfacial shear stress. Increasing u_v results in enhanced bulk turbulence, and therefore a variation in u_v or q_w should have a significant impact on the heating surface temperature field as well as the thermal layer temperature profile, which are both believed to control the incipience process. Future investigations should focus on measuring the probability density function of the wall superheat, pdf (ΔT_{sat}) as well as the thermal layer temperature profile. The pdf (ΔT_{sat}) and the thermal layer temperature profile may be useful in assessing the influence of spatial nonuniformities of ΔT_{sat} on n/A and in providing insight into possible interactions of micro- and macroconvection.

Acknowledgments

This material is based on work supported by the National Science Foundation under Grant No. CTS-9008269. The many useful suggestions provided by Professors B. T. Chao and R. Mei during the course of this work are greatly appreciated.

References

Andritsos, N., and Hanratty, T. J., 1987, "Influence of Interfacial Waves in Stratified Gas-Liquid Flows," *AIChE J.*, Vol. 33, No. 3, pp. 444-454.

Bergles, A. E., and Rohsenow, W. M., 1964, "The Determination of Forced-Convection Surface-Boiling Heat Transfer," *ASME JOURNAL OF HEAT TRANSFER*, Vol. 86, pp. 365-372.

Calka, A., and Judd, R. L., 1985, "Some Aspects of the Interaction Among Nucleation Sites During Saturated Nucleate Boiling," *Int. J. Heat Mass Transfer*, Vol. 28, No. 12, pp. 2331-2341.

Chen, J. C., 1966, "Correlation for Boiling Heat Transfer to Saturated Fluids in Convective Flow," *I&EC Process Design and Development*, Vol. 5, No. 3, pp. 322-329.

Clark, H. B., Strenge, P. S., and Westwater, J. W., 1959, "Active Sites for Nucleate Boiling," *Chem. Eng. Progress Symp. Series*, Vol. 55, No. 29, pp. 103-110.

Eddington, R. I., Kenning, D. B. R., and Korneichev, A. I., 1977, "Comparison of Gas and Vapor Bubble Nucleation on a Brass Surface in Water," *Int. J. Heat Mass Transfer*, Vol. 21, pp. 855-862.

Eddington, R. I., and Kenning, D. B. R., 1978, "The Prediction of Flow Boiling Bubble Populations From Gas Bubble Nucleation Experiments," *Proc. 6th Int. Heat Transfer Conf.*, Vol. 1, pp. 275-280.

Gaertner, R. F., and Westwater, J. W., 1960, "Population of Active Sites in Nucleate Boiling Heat Transfer," *Chem. Eng. Progress Symp. Series*, Vol. 56, No. 30, pp. 39-48.

Gaertner, R. F., 1963, "Distribution of Active Sites in the Nucleate Boiling of Liquids," *Chem. Eng. Progress Symp. Series*, Vol. 59, No. 41, pp. 52-61.

Gaertner, R. F., 1965, "Photographic Study of Nucleate Pool Boiling on a Horizontal Surface," *ASME JOURNAL OF HEAT TRANSFER*, Vol. 87, pp. 17-29.

Griffith, P., and Wallis, J. D., 1960, "The Role of Surface Conditions in Nucleate Boiling," *Chem. Eng. Progress Symp. Series*, No. 30, Vol. 56, pp. 49-63.

Gungor, K. E., and Winterton, R. H. S., 1986, "A General Correlation for Flow Boiling in Tubes and Annuli," *Int. J. Heat Mass Transfer*, Vol. 29, No. 3, pp. 351-358.

Hsu, Y. Y., 1962, "On the Size Range of Active Nucleation Cavities on a Heating Surface," *ASME JOURNAL OF HEAT TRANSFER*, Vol. 98C, pp. 207-216.

Kenning, D. B. R., 1991, "Wall Temperature Patterns in Nucleate Boiling," Technical Report OUEL 1867/91, University of Oxford, Oxford, United Kingdom.

Klausner, J. F., Mei, R., Bernhard, D. M., and Zeng, L. Z., 1992a, "Vapor Bubble Departure in Forced Convection Boiling," *Int. J. Heat Mass Transfer*, in press.

Klausner, J. F., Zeng, L. Z., and Bernhard, D. M., 1992b, "Development of a Film Thickness Probe Using Capacitance for Asymmetrical Two-Phase Flow With Heat Addition," *Rev. Sci. Instrum.*, Vol. 63, No. 5, pp. 3147-3152.

Kurihara, H. M., and Meyers, J. E., 1960, "The Effects of Superheat and Surface Roughness on Boiling Coefficients," *AIChE J.*, Vol. 6, No. 1, pp. 83-91.

Mesler, R. B., 1976, "A Mechanism Supported by Extensive Experimental Evidence to Explain High Heat Fluxes Observed During Nucleate Boiling," *AIChE J.*, Vol. 22, No. 2, pp. 246-252.

Moore, F. M., and Mesler, R. B., 1961, "The Measurement of Rapid Surface Temperature Fluctuations During Nucleate Boiling of Water," *AIChE J.*, Vol. 7, No. 4, pp. 620-624.

Nishikawa, K., Kusuda, H., Yamasaki, K., and Tanaka, K., 1967, "Nucleate Boiling at Low Liquid Levels," *Bulletin of JSME*, Vol. 10, No. 38, pp. 328-338.

Rohsenow, W. M., 1952, "Heat Transfer Symposium," Engineering Research Institute, University of Michigan, Ann Arbor, MI.

Singh, A., Mikic, B. B., and Rohsenow, W. M., 1976, "Active Sites in Boiling," *ASME JOURNAL OF HEAT TRANSFER*, Vol. 98C, pp. 401-406.